JOURNAL OF APPLIED ELECTROCHEMISTRY **26** (1996) 1209–1215

Mass transfer studies at iron felts

D. S. LIZÁRRAGA, J. M. BISANG

Programa de Electroquímica Aplicada e Ingeniería Electroquímica (PRELINE), Facultad de Ingeniería Química, Universidad Nacional del Litoral, Santiago del Estero 2829, 3000 Santa Fe, Argentina

Received 29 September 1995; revised 11 March 1996

Mass transfer has been studied at flow-through iron felts using the reduction of ferricyanide or copper cementation on iron as test reactions. Empirical correlations between a modified Sherwood number and the Reynolds number are proposed. Comparisons of the mass-transfer performance of iron felts with other three-dimensional structures are made.

List of symbols

a_e specific surface area per unit felt volume (m^{-1})
A empty cross-section of the reactor (m^2)
C concentration ($mol\,m^{-3}$)
C_0 inlet concentration ($mol\,m^{-3}$)
d_h hydraulic diameter (m)
e fibre thickness (m)
E electrode potential (V)
D diffusion coefficient ($m^2\,s^{-1}$)
F Faraday constant ($A\,s\,mol^{-1}$)
i current density ($A\,m^{-2}$)
I total current (A)
I_L limiting current (A)
j_m mass transfer j-factor $= (k/v)Sc^{2/3}$
k mass transfer coefficient ($m\,s^{-1}$)
l fibre width (m)
L electrode thickness (m)
Re Reynolds number $= vd_h/\nu$
Re' modified Reynolds number $= vl/\varepsilon\nu$
Sc Schmidt number $= \nu/D$
Sh' modified Sherwood number $= k a_e l^2/D$
t time (s)
T Temperature (K)
v superficial liquid flow velocity ($m\,s^{-1}$)

Greek characters
ε void fraction
μ dynamic viscosity ($kg\,m^{-1}\,s^{-1}$)
ν kinematic viscosity ($m^2\,s^{-1}$)
ν_e charge number of the electrode reaction
ρ iron density ($kg\,m^{-3}$)
ρ_a apparent density of the felt ($kg\,m^{-3}$)
τ_m residence time of the reservoir (s)

1. Introduction

The necessity to treat large solution volumes with small concentration of dangerous species requires the development of reliable and cost-effective processes in order to satisfy the increasing requirements of legal limitations for environmental protection.

Foams and felts are appropriate as materials for purification of waste water, because their structures promote turbulence, enhancing the mass transfer conditions, and at the same time offer high specific surface areas, allowing reactions to take place at appreciable rates. Additionally, the high porosity of these materials produces high permeability for the solution flow and also a low effective electrolyte resistivity, which allows increase in the bed thickness parallel to the current flow. Some authors have proposed the use of foams or felts as electrodes in electrochemical reactors. Thus, Oren and Soffer [1] studied the removal of traces of mercuric ions from aqueous solutions with the use of graphite felt cathode. Oren *et al.* [2, 3] also used fibrous carbon electrodes for the removal of chromium. In [4–6] mass transfer studies at carbon felt electrodes are reported. Tentorio *et al.* [7] studied copper electrodeposition on copper plated polyurethane foams. Nickel foams were appropriately characterized and modelled by Langlois and Coeuret in a series of papers [8–11]. Likewise, Coeuret *et al.* [12, 13] reported the application of nickel foam electrodes in organic electrosynthesis. More recently, Legrand *et al.* [14, 15] produced additional data about the flow behaviour and mass transfer performance of metallic foams in electrochemical reactors of filter press type. Several authors [16–23] performed characterization or applied studies on reticulated vitreous carbon electrodes, which show a similar structure to metallic foams.

In all the above studies three-dimensional structures have been used as electrodes. However, in [24] the use of iron felt for the removal of mercury from chloride solutions by contact deposition is reported. Likewise, Wragg and Bravo de Nahui [25] carried out the cementation of copper with a steel wool-packed cell. The iron felts are easily produced by mechanical means and represent a very versatile material, which can be used either as a reducing agent for the deposition of metal ions, such as mercuric or cupric ions, or as a cheap and efficient electrode material in electrochemical reactors.

The aim of this work is to perform mass transfer studies at iron felts and to compare the mass transfer characteristics with similar materials.

0021-891X

2. Experimental details

Two test reactions were used: (i) electrochemical reduction of ferricyanide at nickel plated electrodes from solutions with $[K_3(CN)_6Fe] \cong 5 \times 10^{-4}$ M, $[K_4(CN)_6Fe] \cong 5 \times 10^{-2}$ M in 1 M NaOH or 3 M NaOH as supporting electrolyte and (ii) copper deposition from dilute $CuSO_4$ solutions by electrochemical displacement using the iron felt as reducing agent.

All the mass transfer studies on felts were performed in a cylindrical reactor, 44.3×10^{-3} m internal diameter and 0.5 m long in a flow circuit system as shown schematically in Fig. 1. The starting material to make the working electrode was commercial iron wool, which was washed for three hours with trichloroethylene in a Soxhlet extraction apparatus in order to remove the slushing compounds. Immediately afterwards the iron wool was compressed to obtain a pellet with an apparent density of approximately 1×10^3 kg m^{-3} and a diameter of 44×10^{-3} m. The porosity of the iron felt was $\varepsilon = 0.87$, calculated as $(\rho - \rho_a)/\rho$ where ρ is the iron density and ρ_a is the apparent density of the felt. The iron felt was plated with nickel by using a plating bath with high throwing power [26]. The porosity of the iron felt plated with nickel was 0.81. Figure 2 shows a micrograph of the nickel plated iron felt. It can be seen that the fibres in the felt have a ribbon shape. The fibre dimensions were determined in 65 cases by optical microscopy. Figure 3 shows a histogram of the width and thickness of the fibres. The mean values are 49×10^{-6} m wide and 28×10^{-6} m thick with standard deviations of 13.7×10^{-6} m and 5.7×10^{-6} m, respectively. Using the mean values of the fibre dimensions and assuming that the felt consists of long and smooth fibres results in a geometric specific surface area of 21300 m^{-1}. The felt thickness was 2.8×10^{-3} m in the experiments for ferricyanide reduction and 4.2×10^{-3} m for copper deposition.

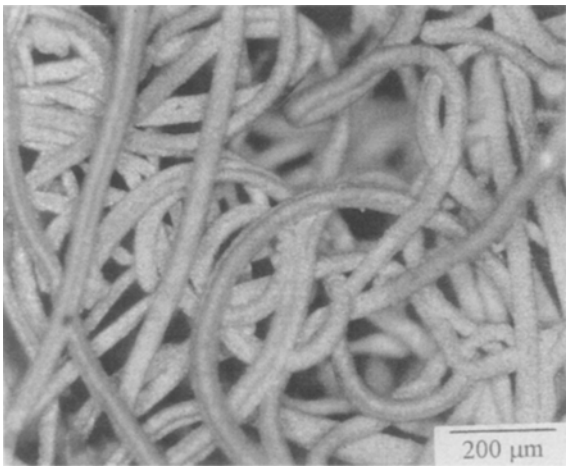

Fig. 2. Micrograph of the nickel plated iron felt. Magnification: ×70.

When the reduction of ferricyanide was the test reaction, the felt electrode was positioned in the central part of the reactor, whose inlet region was filled with 4×10^{-3} m glass beads, in order to achieve developed mass transfer conditions in the felt. As counterelectrode a bundle of nickel-ribbons placed downstream of the working electrode was used. All the experiments were performed under a slow potentiodynamic sweep of 1 mV s^{-1} and the working electrode potential was controlled against a calomel

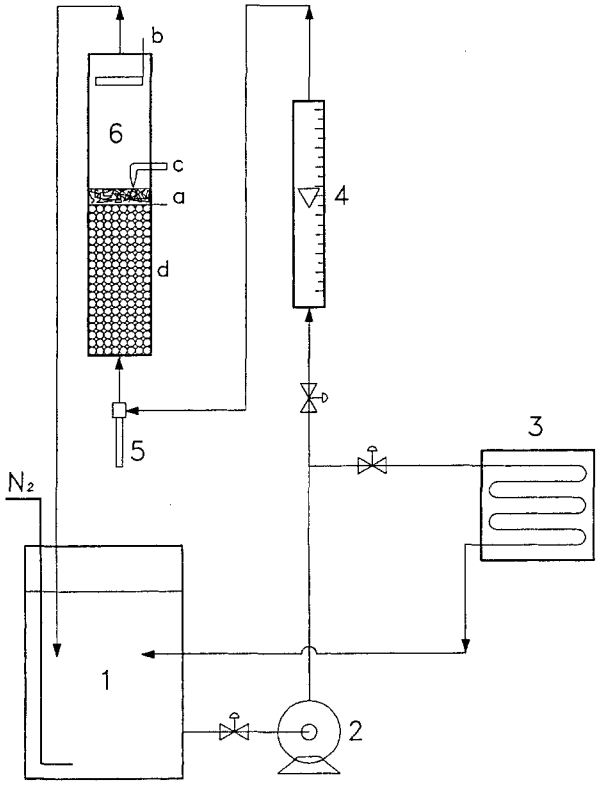

Fig. 1. Schematic view of the experimental setup. (1) Reservoir, (2) pump, (3) thermostat, (4) flow meter, (5) thermometer, (6) reactor. (a) felt electrode, (b) counterelectrode, (c) Luggin capillary, (d) glass beads.

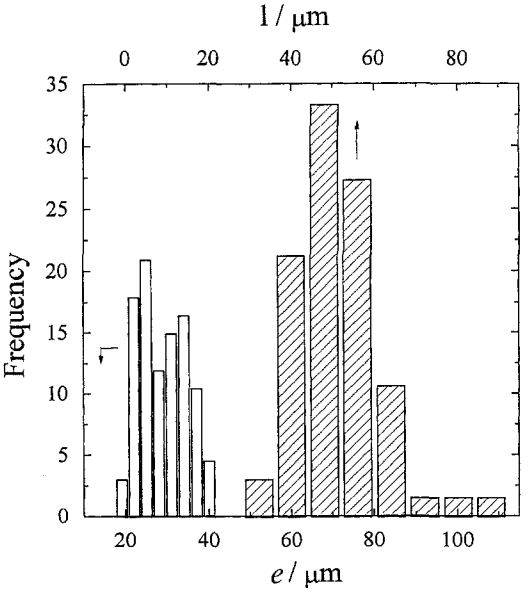

Fig. 3. Distribution of the thickness and width in the nickel plated iron felt.

reference electrode connected to a Luggin capillary positioned in the side of the felt nearest the counter-electrode. For each polarization curve the exact ferricyanide concentration was determined by iodometry [27] with an accuracy of ±2%. Likewise, precautions were adopted in order to reduce the solution decomposition by light, and the solution was frequently replaced. The overall electrolyte volume was 4 dm^3.

When copper deposition was the test reaction, the iron felt worked as reducing agent. Thus, the reactor sketched in Fig. 1 without the counterelectrode was used. The iron felt was placed in the central part of the reactor, whose inlet and outlet regions were filled with glass beads. The starting solution was 1 M Na_2SO_4 with the addition of $CuSO_4$ to achieve a copper concentration of approximately 100 ppm. The overall electrolyte volume was 10 dm^3. During the experiment, small volumes of solution were taken out from the reservoir at different times and the copper concentration was determined using an ion-selective electrode.

All experiments, with both test reactions, were performed at 30 °C and nitrogen was bubbled in the reservoir for 1 h prior to the experiment and during it in order to remove the dissolved oxygen and to promote mixing.

3. Theoretical aspects

For a felt, the interfacial area effective for mass transfer cannot be accurately determined. For this reason the mass transfer rates are reported in terms of transfer coefficients based on a unit volume of felt, ka_e, rather than on a unit of interfacial area, k. This is not a problem because for engineering calculations only the product of k and a_e is necessary. Likewise, the comparison of reactors for waste water treatment is usually performed [28, 29] in terms of the normalized space velocity, which involves the global quantity ka_e.

When the test reaction was ferricyanide reduction, ka_e values were calculated from the limiting current recorded at different flow rates and by using the expression

$$ka_e = -\frac{v}{L}\ln\left(1 - \frac{I_L}{\nu_e F A C_o v}\right) \qquad (1)$$

Equation 1 assumes that the electrochemical reactor can be represented by a plug-flow model and that the current efficiency is 100%.

When the test reaction was copper deposition, the quantity ka_e was determined by following the copper concentration as a function of time and fitting the experimental data with the logarithmic form of the relationship [30]

$$C(t) = C(0)\exp\left\{-\frac{t}{\tau_m}\left[1 - \exp\left(-ka_e\frac{L}{v}\right)\right]\right\} \qquad (2)$$

which assumes that copper deposition is mass-transfer controlled at all times. In Equation 2 the reactor was modelled as a plug-flow system and the reservoir as a well mixed tank.

To lump all the experimental results into a single empirical expression the mass transport data were correlated using the dimensionless relationship

$$Sh' = \text{constant}\ Re'^{\alpha} Sc^{\beta} \qquad (3)$$

The dimensional analysis was performed taking into account the parameters ka_e, ν, v/ε, l, D, as single variables. Thus, the dimensionless numbers are given by

$$Sh' = \frac{ka_e l^2}{D}$$

$$Re' = \frac{v}{\varepsilon}\frac{l}{\nu}$$

$$Sc = \frac{\nu}{D}$$

It must be noted that Equation 3 incorporates a modified Sherwood number based on ka_e as global parameter instead of the mass transfer coefficient as single variable. As characteristic length the mean value of the fibre width was used. In the evaluation of the Reynolds number the use of the interstitial velocity, v/ε was employed. Thus, the void fraction of the felt is considered in the correlation of the experimental results.

4. Results

4.1. *Experiments with rotating disc electrodes*

Prior to the mass-transfer studies at iron felts, the electrochemical behaviour of the test reactions was studied at rotating disc electrodes of nickel for the ferricyanide reduction and copper for copper deposition. Figure 4 shows a set of polarization curves for

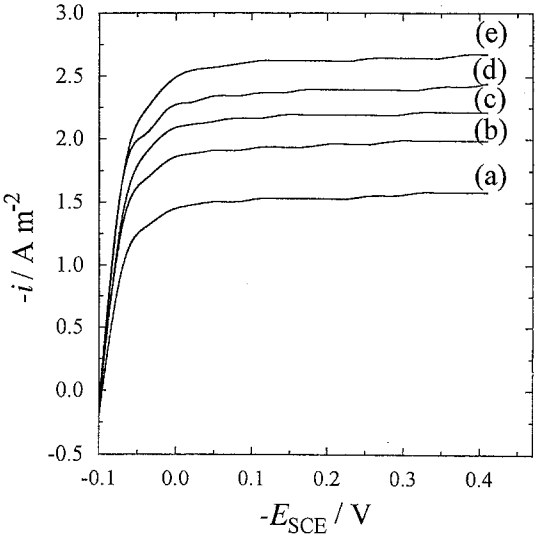

Fig. 4. Current density–potential curves for the reduction of ferricyanide from solutions with $[K_3(CN)_6Fe] = 5 \times 10^{-4}$ M, $[K_4(CN)_6Fe] = 5 \times 10^{-2}$ M in 1 M NaOH as supporting electrolyte at a rotating nickel disc electrode, for rotation rates of: (a) 500, (b) 750, (c) 1000, (d) 1250, (e) 1500 rpm. Potential sweep rate 1 mV s^{-1}.

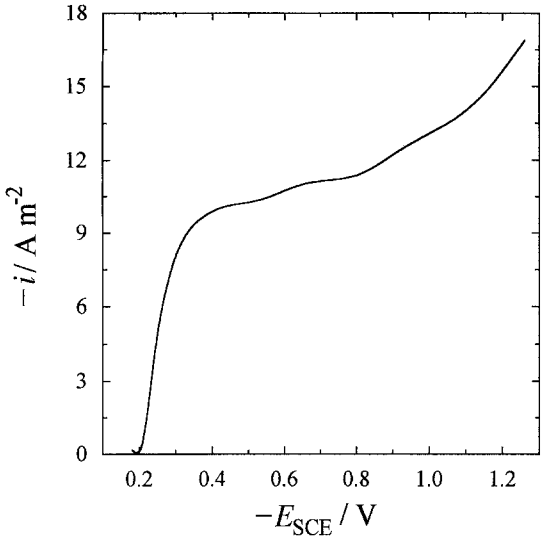

Fig. 5. Current density–potential curve for copper deposition from a 100 pm Cu(II) in 1 M Na_2SO_4 solution at a rotating copper disc electrode. Angular velocity: 1000 rpm.

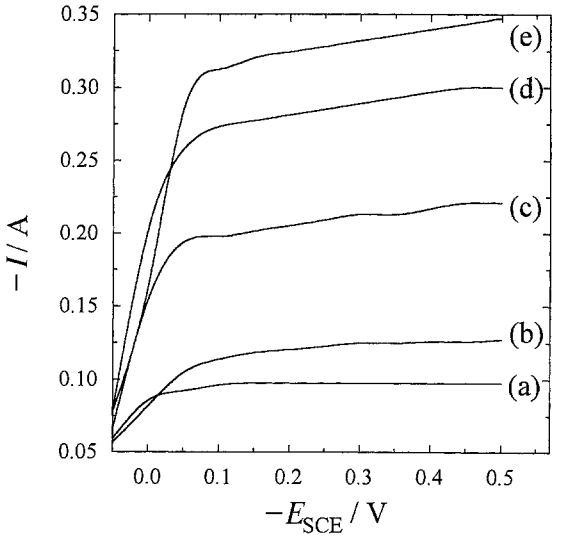

Fig. 6. Current–potential curves for the reduction of ferricyanide from solutions with $[K_3(CN)_6Fe] = 5 \times 10^{-4}$ M, $[K_4(CN)_6Fe] = 5 \times 10^{-2}$ M in 1 M NaOH as supporting electrolyte at a nickel plated iron felt, for superficial liquid flow velocities of: (a) 0.63×10^{-2}, (b) 1.31×10^{-2}, (c) 2.70×10^{-2}, (d) 3.74×10^{-2}, (e) 6.87×10^{-2} m s^{-1}. Potential sweep rate 1 mV s^{-1}.

ferricyanide reduction from 1 M NaOH as supporting electrolyte. Figure 5 shows a polarization curve for copper deposition from a solution containing 100 ppm Cu(II) in 1 M Na_2SO_4 (pH ~ 5) as supporting electrolyte. The potential scan rate was 1 mV s^{-1}. From the limiting current densities, and using the Levich equation, the diffusion coefficients were determined. Table 1 summarizes the composition and physicochemical properties of the solutions. The diffusion coefficient of ferricyanide in 3 M NaOH was calculated from the Stokes–Einstein parameter, $D\mu/T = 2.25 \times 10^{-15}$ kg m s^{-2} K^{-1}, which was determined for 1 M NaOH as supporting electrolyte.

4.2. *Mass-transfer studies at iron felts*

Figure 6 and 7 show some typical current–potential curves for felt electrodes for ferricyanide reduction in 1 M NaOH or 3 M NaOH as supporting electrolyte, respectively. The curves give a well defined limiting current so that ka_e values can be obtained using Equation 1.

Figure 8 shows normalized copper concentration as a function of time at different flow rates. The rest potential of the iron felt in a dilute copper sulfate solution is approximately −0.5 V referred to the saturated calomel electrode. Thus, according to Fig. 5, copper deposition using iron as reducing agent, is mass-transfer controlled, and Equation 2 can be used to calculate ka_e. Figure 8 also shows that at short times, less than 20 min, a linear relationship between $\log C(t)/C(0)$ and time occurs as predicted by Equation 2. But at longer times the copper concentration assymptotes to a constant finite value, approximately 16 ppm after 30 min for $v = 1.82 \times 10^{-2}$ m s^{-1}.

Figure 9 shows the ka_e values as a function of velocity referred to the empty cross-section of the reactor. The correlation of the experimental results yields the following expressions:

$$\text{Ferricyanide reduction, [NaOH]} = 1\text{ M:} \quad ka_e = 7.46\,v^{0.53} \tag{4}$$

$$\text{Ferricyanide reduction, [NaOH]} = 3\text{ M:} \quad ka_e = 6.96\,v^{0.59} \tag{5}$$

$$\text{Copper deposition} \quad ka_e = 17.09\,v^{0.49} \tag{6}$$

where the units of ka_e are s^{-1} and those of v are m s^{-1}.

In equations 4 to 6 the exponents of the velocity are close with a mean value of 0.54, which is very close to exponents previously reported [5, 7, 15], but the constants differ primarily due to the different physicochemical properties of the solutions.

Table 1. Properties of electrolytes

Composition	$[K_3(CN)_6Fe] = 5 \times 10^{-4}$ M $[K_4(CN)_6Fe] = 5 \times 10^{-2}$ M $[NaOH] = 1$ M	$[K_3(CN)_6Fe] = 5 \times 10^{-4}$ M $[K_4(CN)_6Fe] = 5 \times 10^{-2}$ M $[NaOH] = 3$ M	$[Cu^{2+}] = 100\,ppm$ $[Na_2SO_4] = 1$ M $pH \sim 5$
Density/kg m^{-3}	1.05×10^3	1.12×10^3	1.11×10^3
Dynamic viscosity/kg m^{-1} s^{-1}	1.12×10^{-3}	1.55×10^{-3}	1.24×10^{-3}
Kinematic viscosity/m^2 s^{-1}	1.07×10^{-6}	1.38×10^{-6}	1.11×10^{-6}
Diffusion coefficient/m^2 s^{-1}	6.09×10^{-10}	4.40×10^{-10}	4.14×10^{-10}
Sc	1757	3136	2681

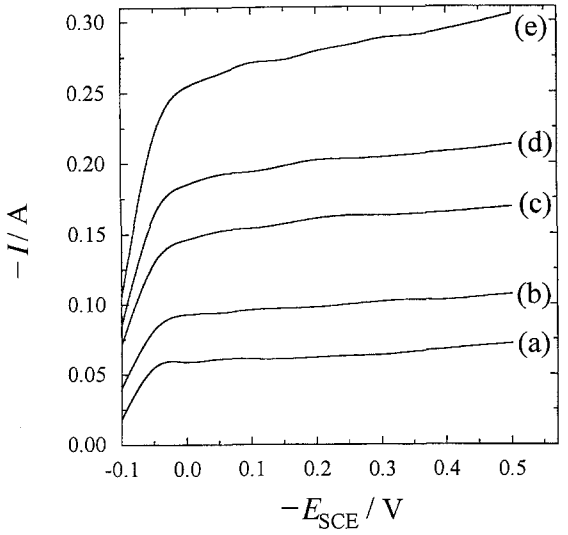

Fig. 7. Current–potential curves for the reduction of ferricyanide from solutions with $[K_3(CN)_6Fe] = 5 \times 10^{-4}$ M, $[K_4(CN)_6Fe] = 5 \times 10^{-2}$ M in 3 M NaOH as supporting electrolyte at a nickel plated iron felt, for superficial liquid flow velocities of: (a) 0.63×10^{-2}, (b) 1.31×10^{-2}, (c) 2.70×10^{-2}, (d) 3.74×10^{-2}, (e) 6.78×10^{-2} m s^{-1}. Potential sweep rate 1 mV s^{-1}.

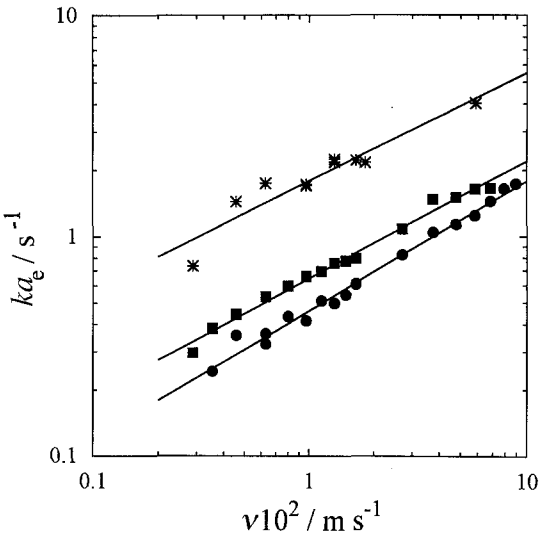

Fig. 9. Variation of ka_e with the superficial liquid flow velocity. (■) Ferricyanide reduction in 1 M NaOH, (●) ferricyanide reduction in 3 M NaOH, (*) copper deposition from a 100 ppm Cu(II) in 1 M Na_2SO_4 solution using the iron felt as reducing agent.

Assuming the usual value of 1/3 for the exponent in the Schmidt number in Equation 3, the experimental data are plotted in dimensionless form in Figure 10. Also included, using the symbol (○), is a value obtained in previous work [24], where an iron felt was used as reducing agent for the removal of mercuric ions, $Sc = 543$. It can be observed that the experimental results for electrochemical reduction of ferricyanide and mercury deposition are in close agreement in spite of the difference in Schmidt number. Using the least squares method to correlate the data results in

$$Sh' = 0.28\, Re'^{0.56} Sc^{1/3} \qquad (7)$$

with a linear correlation coefficient of 0.9851. Figure 10 shows that the data for copper deposition have the same slope but are 3.7 times higher. Data are represented by

$$Sh' = 1.04\, Re'^{0.49} Sc^{1/3} \qquad (8)$$

with a linear correlation coefficient of 0.9496. Similar behaviour was found by Wragg *et al.* [31, 32] and recently by Podlaha and Fenton [23]. In order to explain this discrepancy, additional experiments with a copper rotating disc were performed. Figure 11 shows the current as a function of time under potentiostatic conditions for copper deposition from 100 ppm Cu(II) in 1 M Na_2SO_4 as supporting electrolyte. It can be observed that, in spite of the low level of copper concentration, the current increases with time. Thus, at 30 min of operation the current becomes twice its initial value due to the increase in

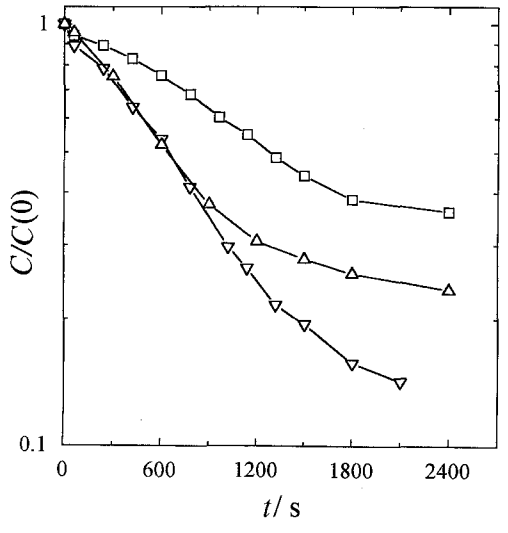

Fig. 8. Logarithm of normalized copper concentration against time curves. Solution: 100 ppm Cu(II) in 1 M Na_2SO_4. Superficial liquid flow velocities: (□) 0.46×10^{-2}, (△) 1.31×10^{-2}, (▽) 1.82×10^{-2} m s^{-1}.

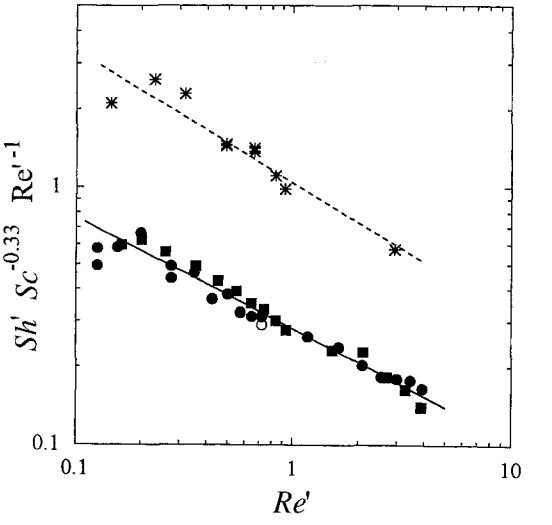

Fig. 10. Modified Sherwood–Reynolds correlations for iron felts. (■) Ferricyanide reduction in 1 M NaOH, (●) ferricyanide reduction in 3 M NaOH, (○) removal of mercuric ions using the iron felt as reducing agent, (*) copper deposition from a 100 ppm Cu(II) in 1 M Na_2SO_4 solution using the iron felt as reducing agent. Full line: Equation 7. Dashed line: Equation 8.

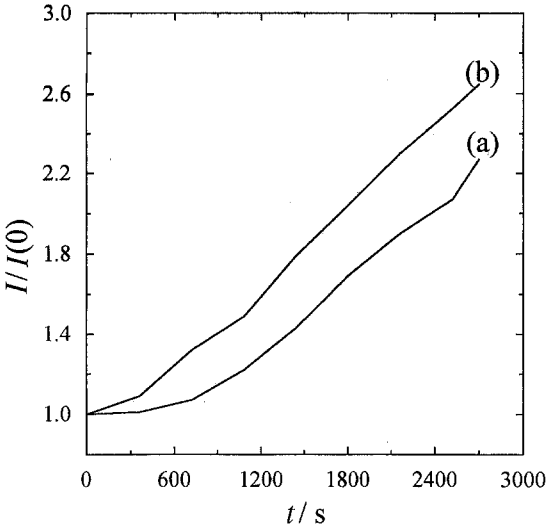

Fig. 11. Variation of the normalized current with time for copper deposition from a 100 ppm Cu(II) in 1 M Na_2SO_4 solution at a rotating copper disc electrode. (a) $E_{SCE} = -0.5$ V, (b) $E_{SCE} = -0.6$ V. Angular velocity: 1000 rpm.

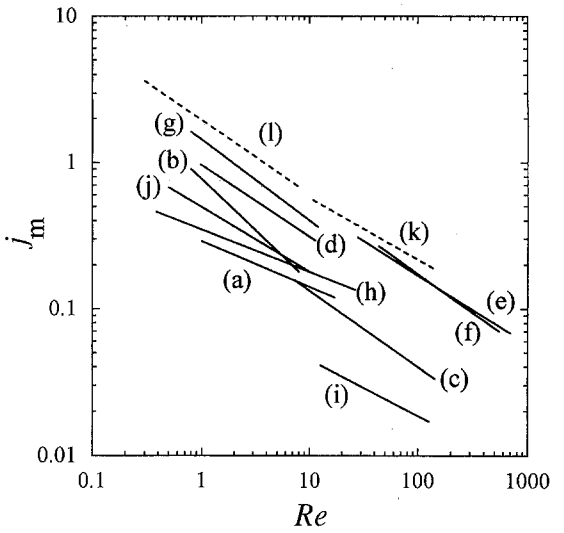

Fig. 12. *j*-Factor as a function of the Reynolds number for different three-dimensional structures. (a) Carbon felts [5]. (b) Nickel foams, 100 pores per inch, flow-through configuration [9], calculated from the informed empirical equation. (c) Reticulated vitreous carbon 100 pores per inch [19], calculated from the informed dimensionless correlation. (d) fluidized bed electrodes [34], calculated from the informed dimensionless correlation with $\varepsilon = 0.552$. (e) Reticulated copper electrodes 10 pores per inch [7], calculated from the informed dimensionless correlation. (f) Reticulated copper electrodes 20 pores per inch [7], calculated from the informed dimensionless correlation. (g) Packed bed electrode [35], calculated from the informed dimensionless correlation with $\varepsilon = 0.4055$, $d_p = 0.635$ cm and $L = 4.1$ cm. (h) Reticulated vitreous carbon electrode, 45 pores per inch [23]. (i) Nickel foams, 60 pores per inch [15]. (j) This work, ferricyanide reduction. (k) Copper cementation on packed bed of iron particles [31]. (l) This work, copper cementation.

electrode roughness. This effect is sharper at higher potentials. A similar behaviour was found by Ibl [33] for copper deposition from more concentrated and acidified copper sulfate solutions. Therefore, the high values of mass transfer, obtained for copper deposition, can be attributed to the increase in the surface area due to metal deposition. Scanning electron microscopy studies [32] have revealed that the surface enhancement is due to the extremely dendritic nature of the cement copper.

5. Comparison with previous studies

To compare the mass transfer data at iron felts with those at other three-dimensional structures such as packed and fluidized beds, carbon felts, nickel foams or reticulated vitreous carbon, a characteristic length must be adopted, which must be common for all the structures. Thus, a convenient form of the characteristic length is the hydraulic diameter defined as:

$$d_h = \frac{4\varepsilon}{a_e} \tag{9}$$

Using the hydraulic diameter results in correlations with dimensionless numbers defined in the conventional form, which permits the comparison of mass-transfer data of similar three-dimensional structures but with some errors introduced by the uncertainty in a_e.

Figure 12 shows the *j*-factor as a function of Reynolds number. Line *j* corresponds to the results of the present work for the ferricyanide reduction as test reaction. It can be observed that the mass-transfer characteristics of iron felts are comparable to those of similar materials. The dashed lines in Fig. 12 correspond to copper cementation. The data of the present work, line l, are in close agreement with previous results, line *k* [31, 32].

6. Conclusions

The results confirm the good mass-transfer performance of felts, which is close to that of similar three-dimensional structures.

Two dimensionless correlations to perform mass transfer calculations in iron felts were obtained. One of them, Equation 7, gives mass-transfer coefficients based on a unit felt volume when the electrode reaction does not alter the electrode surface and the second, Equation 8, is appropriate for metallic deposition processes.

Thus, iron felts are an attractive material for electrochemical applications due to their low cost, high specific surface area and high porosity.

Acknowledgements

This work was supported by the Universidad Nacional del Litoral (CAI + D 94-0858-007-058) and Consejo Nacional de Investigaciones Científicas y Técnicas (CONICET, Argentina). One of us (D.S.E.) is indebted to El Litoral S.R.L. for the fellowship granted.

References

[1] Y. Oren and A. Soffer, *Electrochim. Acta* **28** (1983) 1649.
[2] D. Golub and Y. Oren, *J. Appl. Electrochem.* **19** (1989) 311.
[3] M. Abda, Z. Gavra and Y. Oren, *ibid.* **21** (1991) 734.
[4] D. Schmal, J. Van Erkel and P. J. Van Duin *ibid.* **16** (1986) 422.

[5] R. Carta, S. Palmas, A. M. Polcaro and G. Tola, *ibid.* **21** (1991) 793.
[6] N. Vatistas, P. F. Marconi and M. Bartolozzi, *Electrochim. Acta* **36** (1991) 339.
[7] A. Tentorio, U. Casolo-Ginelli, *J. Appl. Electrochem.* **8** (1978) 195.
[8] S. Langlois and F. Coeuret, *ibid.* **19** (1989) 43.
[9] *Idem, ibid.* **19** (1989) 51.
[10] *Idem, ibid.* **20** (1990) 740.
[11] *Idem, ibid.* **20** (1990) 749.
[12] J. Nanzer, S. Langlois and F. Coeuret, *ibid.* **23** (1993) 471.
[13] *Idem, ibid.* **23** (1993) 447.
[14] A. Montillet, J. Comiti and J. Legrand, *ibid.* **23** (1993) 1045.
[15] A. Montillet, J. Comiti and J. Legrand, *ibid.* **24** (1994) 384.
[16] J. Wang, *Electrochim. Acta* **26** (1981) 1721.
[17] J. Wang and H. D. Dewald, *J. Electrochem. Soc.* **130** (1983) 1814.
[18] M. Matlosz and J. Newman, *ibid.* **133** (1986) 1850.
[19] D. Pletcher, I. Whyte, F. C. Walsh and J. P. Millington, *J.Appl. Electrochem.* **21** (1991) 659.
[20] *Idem, ibid.* **21** (1991) 667.
[21] *Idem, J. Chem. Tech. Biotechnol.* **55** (1992) 147.
[22] *Idem, J. Appl. Electrochem.* **23** (1993) 82.
[23] E. J. Podlaha and J. M. Fenton, *ibid.* **25** (1995) 299.
[24] J. M. Grau and J. M. Bisang, *J. Chem. Tech. Biotechnol.* **62** (1995) 153.
[25] A. A. Wragg and F. N. Bravo de Nahui, *I. Chem. E. Symp. Ser.* **127** (1992) 141.
[26] H. Brown and B. B. Knapp, *in* 'Modern Electroplating' 3rd edn. (edited by F. A. Lowenheim), John Wiley & Sons, New York (1974) Ch. 12, p. 292.
[27] I. M. Kolthoff, E. B. Sandell, E. J. Meehan and S. Bruckenstein, 'Quantitative Chemical Analysis', 4th edn., MacMillan, New York (1969).
[28] G. Kreysa, *Electrochim. Acta* **26** (1981) 1693.
[29] F. C. Walsh, *ibid.* **38**, (1993) 465.
[30] A. T. S. Walker and A. A. Wragg, *Electrochim. Acta* **22** (1977) 1129.
[31] F. Bravo de Nahui and A. A. Wragg, Extended Abstracts, ISE 36th Meeting, Salamanca, Spain (1985), paper 4050.
[32] F. Bravo de Nahui, R. M. Hooper and A. A. Wragg, *Chemistry and Industry* 1st Sept. (1986) 571.
[33] N. Ibl and K. Schadegg, *J. Electrochem. Soc* **114** (1967) 54.
[34] A. T. S. Walker and A. A. Wragg, *Electrochim. Acta* **25** (1980) 323.
[35] R. Alkire, B. Gracon, T. Grueter, J. Marek and P. Blackburn, *J. Electrochem. Soc.* **127** (1980) 1085.